

## Research Paper

# Anti-tumor Effect of Integrin Targeted $^{177}\text{Lu}$ -3PRGD<sub>2</sub> and Combined Therapy with Endostar

Jiyun Shi<sup>1,2</sup>, Di Fan<sup>1,3</sup>, Chengyan Dong<sup>1,3</sup>, Hao Liu<sup>1,3</sup>, Bing Jia<sup>1,3</sup>, Huiyun Zhao<sup>1,2</sup>, Xiaona Jin<sup>4</sup>, Zhaofei Liu<sup>1,3</sup>, Fang Li<sup>4</sup>, Fan Wang<sup>1,3</sup>✉

1. Medical Isotopes Research Center, Peking University, Beijing 100191, China;
2. Medical and Healthy Analytical Center, Peking University, Beijing 100191, China;
3. Department of Radiation Medicine, Basic Medical Sciences, Peking University, Beijing 100191, China;
4. Department of Nuclear Medicine, Peking Union Medical College Hospital, Beijing 100857, China.

✉ Corresponding author: Fan Wang, Ph.D., Medical Isotopes Research Center, Peking University, 38 Xueyuan Rd, Beijing 100191, China. Tel.: 86-10-82802871 & Fax: 86-10-82801145. E-mail: wangfan@bjmu.edu.cn.

© Ivyspring International Publisher. This is an open-access article distributed under the terms of the Creative Commons License (<http://creativecommons.org/licenses/by-nc-nd/3.0/>). Reproduction is permitted for personal, noncommercial use, provided that the article is in whole, unmodified, and properly cited.

Received: 2013.09.29; Accepted: 2013.12.04; Published: 2014.01.18

## Abstract

**Purpose:** Targeted radiotherapy (TRT) is an emerging approach for tumor treatment. Previously, 3PRGD<sub>2</sub> (a dimeric RGD peptide with 3 PEG<sub>4</sub> linkers) has been demonstrated to be of advantage for integrin  $\alpha_v\beta_3$  targeting. Given the promising results of  $^{99m}\text{Tc}$ -3PRGD<sub>2</sub> for lung cancer detection in human beings, we are encouraged to investigate the radiotherapeutic efficacy of radiolabeled 3PRGD<sub>2</sub>. The goal of this study was to investigate and optimize the integrin  $\alpha_v\beta_3$  mediated therapeutic effect of  $^{177}\text{Lu}$ -3PRGD<sub>2</sub> in the animal model.

**Experimental Design:** Biodistribution, gamma imaging and maximum tolerated dose (MTD) studies of  $^{177}\text{Lu}$ -3PRGD<sub>2</sub> were performed. The targeted radiotherapy (TRT) with single dose and repeated doses as well as the combined therapy of TRT and the anti-angiogenic therapy (AAT) with Endostar were conducted in U87MG tumor model. The hematoxylin and eosin (H&E) staining and immunochemistry (IHC) were performed post-treatment to evaluate the therapeutic effect.

**Results:** The U87MG tumor uptake of  $^{177}\text{Lu}$ -3PRGD<sub>2</sub> was relatively high ( $6.03 \pm 0.65$  %ID/g,  $4.62 \pm 1.44$  %ID/g,  $3.55 \pm 1.08$  %ID/g, and  $1.22 \pm 0.18$  %ID/g at 1 h, 4 h, 24 h, and 72 h postinjection, respectively), and the gamma imaging could visualize the tumors clearly. The MTD of  $^{177}\text{Lu}$ -3PRGD<sub>2</sub> in nude mice ( $>111$  MBq) was twice to that of  $^{90}\text{Y}$ -3PRGD<sub>2</sub> (55.5 MBq). U87MG tumor growth was significantly delayed by  $^{177}\text{Lu}$ -3PRGD<sub>2</sub> TRT. Significantly increased anti-tumor effects were observed in the two doses or combined treatment groups.

**Conclusion:** The two-dose TRT and combined therapy with Endostar potently enhanced the tumor growth inhibition, but the former does not need to inject daily for weeks, avoiding a lot of unnecessary inconvenience and suffering for patients, which could potentially be rapidly translated into clinical practice in the future.

Key words: Integrin  $\alpha_v\beta_3$ , Arg-Gly-Asp (RGD),  $^{177}\text{Lu}$ , radionuclide therapy, combination therapy.

## Introduction

Radiotherapy is a very important tool in the fight against cancer and is used in the treatment of as many as 50% of all cancer patients (1-3). Compared with the conventional radiotherapy, the targeted radiotherapy

(TRT) is an emerging approach for tumor treatment, which delivers the radiation in a targeted manner by a ligand that specifically binds to receptors overexpressed on the surface of some cancerous cells, thus

providing good efficacy and tolerability outcomes (4-7).

Integrin  $\alpha_v\beta_3$  is highly expressed on some tumor cells and new-born vessels, but is absent in resting vessels and most normal organ systems, making it a very attractive target for both tumor cell and tumor vasculature targeted imaging and therapy (8-10). Integrin  $\alpha_v\beta_3$  has been proven to specifically recognize Arg-Gly-Asp (RGD) tripeptide sequence. In the last 20 years, a series of RGD peptide-based probes have been intensively developed for multimodality molecular imaging of integrin  $\alpha_v\beta_3$ -positive tumors (11-15). However, the RGD-based targeted radionuclide therapy is typically rare. Janssen ML *et al.* reported, for the first time, the integrin  $\alpha_v\beta_3$  targeted radionuclide therapy with  $^{90}\text{Y}$ -labeled dimeric RGD peptide E[c(RGDfK)]<sub>2</sub> in the NIH:OVCAR-3 subcutaneous (s.c.) ovarian carcinoma-bearing nude mouse model. A single injection of 37 MBq of  $^{90}\text{Y}$ -DOTA-E[c(RGDfK)]<sub>2</sub> caused a significant tumor growth delay in treatment group as compared with the untreated control group (16).

Since a promising TRT relies on the maximized radiation accumulation and retention in tumors while minimizing the exposure of radiolabeled agents to normal tissues, many attempts, including multivalency and PEGylation, have been made to pursue more ideal RGD probes with high tumor targeting capability (17-19). We have combined both multivalency and PEGylation concepts together and developed a series of new RGD dimers with PEG<sub>4</sub> and Gly<sub>3</sub> linkers (e.g. 3PRGD<sub>2</sub>, a dimeric RGD peptide with 3 PEG<sub>4</sub> linkers, see Fig 1) (20-24). The previous result showed that the 3PRGD<sub>2</sub> conjugate (DOTA-3PRGD<sub>2</sub>, IC<sub>50</sub> = 1.25 ± 0.16 nM) had higher binding affinity to integrin  $\alpha_v\beta_3$  than the RGD monomer (c(RGDyK), IC<sub>50</sub> = 49.89 ± 3.63 nM) and RGD dimer conjugates

(DOTA-RGD<sub>2</sub>, IC<sub>50</sub> = 8.02 ± 1.94 nM). The radiolabeled 3PRGD<sub>2</sub> resulted in a high tumor uptake and improved in vivo pharmacokinetics as compared with those conventional RGD multimers, including RGD dimer (RGD<sub>2</sub>) and tetramer (RGD<sub>4</sub>), which simply utilized the multivalency concept to increase the tumor uptake (15, 17-21, 24). Furthermore, kit-formulated  $^{99\text{m}}\text{Tc}$ -3PRGD<sub>2</sub> has been successfully applied in clinic for characterization of malignant solitary pulmonary nodules (SPNs) (25), identification of differentiated thyroid cancer (DTC) patients with radioactive iodine-refractory (RAIR) lesions (26), and detection of lung cancer (27). Given the promising results of  $^{99\text{m}}\text{Tc}$ -3PRGD<sub>2</sub> for imaging in clinic, we were encouraged to further investigate the radiotherapeutic efficacy of radiolabeled 3PRGD<sub>2</sub>. In our previous research,  $^{90}\text{Y}$ -3PRGD<sub>2</sub> showed comparable tumor growth inhibition but significantly lower toxicity as the lower accumulation in normal organs in comparison of  $^{90}\text{Y}$ -RGD<sub>4</sub> (24), indicating that the TRT of radiolabeled 3PRGD<sub>2</sub> merits further investigation to achieve the better radiotherapeutic efficacy.

$^{177}\text{Lu}$ , with longer half-life of 6.7 days and relatively mild  $\beta$ -emission (E<sub>max</sub>: 0.497 MeV), offers the advantages to achieve higher injected dose amount and longer retention of radiation in tumors but lower irradiation of normal tissues adjacent to the tumors as compared with  $^{90}\text{Y}$  (half-life: 2.67 d, E<sub>max</sub>: 2.28 MeV). Moreover, the  $\gamma$ -emission of  $^{177}\text{Lu}$  enables its use for the imaging and dosimetry assessment of patients before and during treatment without requiring a surrogate tracer. In this study,  $^{177}\text{Lu}$  radiolabeled 3PRGD<sub>2</sub> was first investigated in terms of Glioblastoma multiforme (GBM) targeting capability and imaging feasibility, and was then examined in a therapeutic efficacy study on single dose as well as two-dose regimen TRT in a GBM animal model.

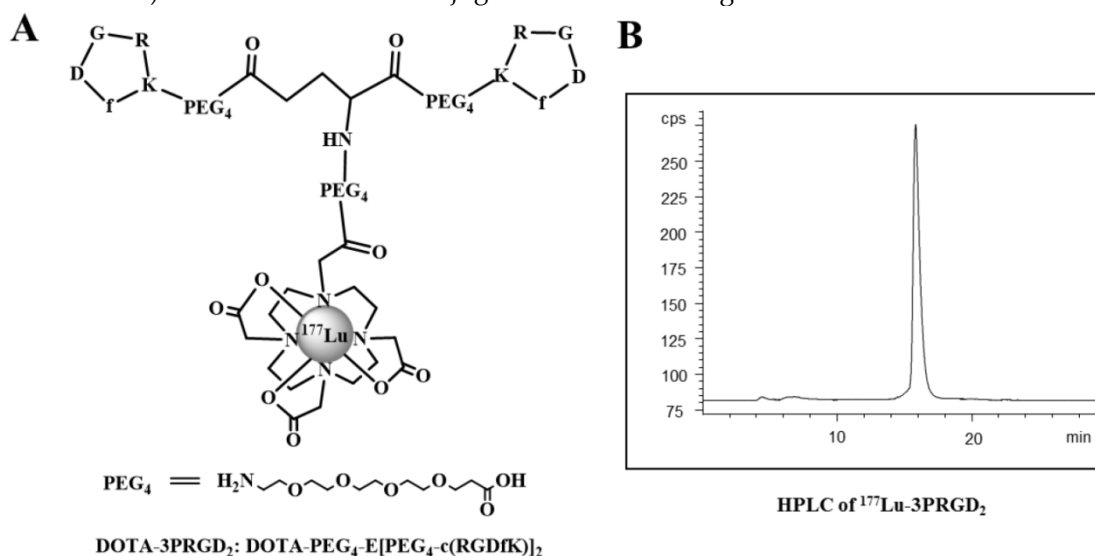


**Figure 1.** The chemical structure (A) and HPLC chromatography (B) of  $^{177}\text{Lu}$ -3PRGD<sub>2</sub>.

Angiogenesis is a key early event in tumor progression and metastasis. The inhibition of tumor growth by anti-angiogenic drugs has been achieved both in preclinical studies and in clinical trials, where promising anti-tumor responses have been reported for a variety of anti-angiogenic agents (28). Endostar, a novel recombinant human endostatin, which was approved by the China Food and Drug Administration (CFDA) in 2005 for clinical applications, showed strong growth inhibition of a variety of murine and xenotransplanted human tumors by suppressing neovascularization (29-31). The combination of radiotherapy and chemotherapy is an appealing approach that has led to improved treatment results in patients with advanced solid tumors (32-35). Herein, the combination therapy employing  $^{177}\text{Lu}$ -3PRGD<sub>2</sub> TRT and Endostar anti-angiogenic therapy (AAT) was utilized to treat U87MG glioblastoma in a mouse model. Our aim was to optimize the therapeutic effect of radio-labeled 3PRGD<sub>2</sub> for TRT of integrin  $\alpha_v\beta_3$ -positive tumors.

## Materials and Methods

### Materials

All commercially available chemical reagents were of analytical grade and used without further purification. See the supplemental material for the details.

### Preparation of $^{177}\text{Lu}$ -3PRGD<sub>2</sub>

The 3PRGD<sub>2</sub> peptide was conjugated with chelator DOTA using previously described method (15). For  $^{177}\text{Lu}$  radiolabeling, 3700 MBq of  $^{177}\text{Lu}$  was diluted in 100  $\mu\text{L}$  0.4 M sodium acetate buffer (pH 5.0), and added to 50  $\mu\text{g}$  DOTA-3PRGD<sub>2</sub> conjugate (1  $\mu\text{g}/\mu\text{L}$  in water) in a 1.5 mL eppendorf tube. The reaction tube was incubated in air bath for 10 min at 100 °C, and the  $^{177}\text{Lu}$  labeled peptide was then purified by the Sep-Pak C-18 cartridge. The quality control (QC) of the tracer was carried out with radio-HPLC by the previously reported method (15). The purified product was dissolved in saline and passed through a 0.22  $\mu\text{m}$  syringe filter for in vivo animal experiments.

### Cell culture and animal model

U87MG human glioblastoma cells were obtained from American Type Culture Collection (Manassas, VA). U87MG tumor model was established by subcutaneous injection of  $2 \times 10^6$  U87MG tumor cells into the right thighs. All animal experiments were performed in accordance with guidelines of Institutional Animal Care and Use Committee of Peking University. See the supplemental material for the detailed procedures.

### Biodistribution studies

Female nude mice bearing U87MG xenografts (4 mice per group) were injected with 370 kBq of  $^{177}\text{Lu}$ -3PRGD<sub>2</sub> via tail vein to evaluate the distribution in major organs. The mice were sacrificed at 1 h, 4 h, 24 h and 72 h postinjection (p.i.). Blood, heart, liver, spleen, kidney, brain, lung, intestine, muscle, bone and tumor were harvested, weighed, and measured for radioactivity in a  $\gamma$ -counter (Wallac 1470-002, Perkin-Elmer, Finland). A group of four U87MG tumor-bearing nude mice was co-injected with 350  $\mu\text{g}$  of c(RGDyK) for blocking study, and the biodistribution was performed at 1 h p.i. using the same method. Another group of four U87MG tumor-bearing nude mice was injected with 370 kBq of  $^{177}\text{Lu}$ -3PRGD<sub>2</sub> following with 3 days of intraperitoneal Endostar administration (8 mg/kg per day), then the biodistribution was performed at 72 h p.i. using the above method. Organ uptake was calculated as the percentage of injected dose per gram of tissue (%ID/g). Values were expressed as mean  $\pm$  SD (n = 4/group).

### Gamma imaging

For the planar  $\gamma$ -imaging, the U87MG tumor-bearing nude mice were anesthetized with an intraperitoneal injection of sodium pentobarbital at a dose of 45.0 mg/kg. Each animal was administered with  $\sim 74$  MBq of  $^{177}\text{Lu}$ -3PRGD<sub>2</sub> in 0.2 mL of saline (n = 3 per group). Animals were placed on a two-head  $\gamma$ -camera (GE Infinia Hawkeye) equipped with a parallel-hole, low-energy, and high-resolution collimator. Images were acquired at 4 h and 24 h p.i., and stored digitally in a 128 $\times$ 128 matrix. The acquisition count limits were set at 500 k counts.

### Maximum tolerated dose studies

The maximum tolerated dose (MTD) of  $^{177}\text{Lu}$ -3PRGD<sub>2</sub> in non-tumor-bearing female BALB/c nude mice was determined by intravenous injection of escalating activities of  $^{177}\text{Lu}$ -3PRGD<sub>2</sub> (37, 74 and 111 MBq per mouse), respectively (n = 7 per group). Body weight and health status were determined twice weekly over 20 days. Peripheral blood was collected from the tail vein twice weekly and then tested in a blood analyzer for white blood cell (WBC), red blood cell (RBC), hemoglobin (HGB), platelet (PLT) and neutrophil granulocyte (GRN) counts, etc. The MTD was set below the dose that caused severe loss of body weight (>20% of original weight), or death of one or more animals of a dose group.

### Targeted radiotherapy and combined therapy

To assess the therapeutic potential of  $^{177}\text{Lu}$ -3PRGD<sub>2</sub>, U87MG tumor-bearing nude mice with a tumor size of  $\sim 50$  mm<sup>3</sup> were randomly assigned to

several groups ( $n = 9$  mice per group). Control group was injected via tail vein with single dose injection of saline. For TRT, U87MG tumor mice were dosed intravenously with either a single injection of 0.2 mL of  $^{177}\text{Lu}$ -3PRGD<sub>2</sub> (5.55 GBq/kg; 111.0 MBq/0.2 mL; peptide 1.5  $\mu\text{g}$ ) or 2 equal doses on day 0 and day 6 (cumulative dose, 111.0 MBq/0.2 mL $\times$ 2; peptide 1.5  $\mu\text{g}$ /injection).

For the combination of TRT and AAT, a single dose injection of  $^{177}\text{Lu}$ -3PRGD<sub>2</sub> (111 MBq) on day 0 combined with once daily administration of Endostar (8 mg/kg peritumoral subcutaneous (s.c.) injection) for 2 weeks (day 0 - 13). Furthermore, a scheduled dose injection of  $^{177}\text{Lu}$ -3PRGD<sub>2</sub> (111 MBq) on day 5 combined with pretreatment of once daily administration of Endostar (8 mg/kg s.c. injection) for 5 days, then the Endostar treatment was continued for a total of 2 weeks (day 0 - 13).

Tumor dimensions were measured twice weekly with digital calipers, and the tumor volume was calculated using the formula: volume = 1/2 (length  $\times$  width  $\times$  width) (36). To monitor potential toxicity, body weight was measured. Mice were euthanized when the tumor size exceeded the volume of 1,500 mm<sup>3</sup> or the body weight lost >20% of original weight.

### Histopathology and immunohistochemistry

Frozen U87MG tumor tissues were cryo-sectioned and evaluated by standard hematoxylin and eosin (H&E) staining and immunohistochemistry (IHC). See the supplemental material for the detailed procedures.

### Statistical analysis

Quantitative data are expressed as means  $\pm$  SD. Means were compared using one-way analysis of variance (ANOVA) and Student's *t* test. *P* values <0.05 were considered statistically significant.

## Results

### Preparation of $^{177}\text{Lu}$ -3PRGD<sub>2</sub>

After radiolabeling and purification, the specific activity of  $^{177}\text{Lu}$  tracer was typically about 7.4-14.8 MBq/nmol (0.2-0.4 Ci/mmol), with radiochemical purity greater than 99.5% (labeling yield more than 95%) as determined by analytic radio-HPLC.

### Tumor uptake of $^{177}\text{Lu}$ -3PRGD<sub>2</sub>

In biodistribution studies, the  $^{177}\text{Lu}$ -3PRGD<sub>2</sub> depicted a similar biodistribution pattern with previously reported  $^{111}\text{In}$ -3PRGD<sub>2</sub>, which represents for  $^{90}\text{Y}$ -3PRGD<sub>2</sub> (24). As shown in Fig 2A, the uptake of  $^{177}\text{Lu}$ -3PRGD<sub>2</sub> in U87MG tumors was  $6.03 \pm 0.65$  %ID/g at 1 h p.i., which was decreased to  $4.62 \pm 1.44$  %ID/g,  $3.55 \pm 1.08$  %ID/g, and  $1.22 \pm 0.18$  %ID/g at 4

h, 24 h, and 72 h p.i., respectively ( $n = 4$ /group). The %ID/g data are available as supplementary material (Table S1).  $^{177}\text{Lu}$ -3PRGD<sub>2</sub> showed rapid blood clearance, and was cleared predominantly through both gastrointestinal and renal pathways as evidenced by relatively high intestine uptake ( $5.16 \pm 0.48$  %ID/g and  $4.15 \pm 1.12$  %ID/g) and kidney uptake ( $4.18 \pm 1.08$  %ID/g and  $3.13 \pm 0.59$  %ID/g) at 1 h and 4 h p.i., respectively. The tumor uptake of  $^{177}\text{Lu}$ -3PRGD<sub>2</sub> was significantly inhibited by co-injection of the excess cold RGD peptide in blocking study ( $P < 0.001$ , Fig 2C, Supplementary Material: Table S1), indicating the receptor-mediated targeting of  $^{177}\text{Lu}$ -3PRGD<sub>2</sub> in integrin-positive U87MG tumors.

The influence of anti-angiogenic therapy with Endostar on  $^{177}\text{Lu}$ -3PRGD<sub>2</sub> tumor uptake was also determined. No difference on the tumor uptake was observed between the treatment and no-treatment groups (Fig 2D,  $P > 0.5$ ). The result may suggest that the  $^{177}\text{Lu}$ -3PRGD<sub>2</sub> and Endostar do not bind to and work on the same receptor, although the binding mechanism of Endostar at the molecular level is unclear.

In planar  $\gamma$ -imaging study, the U87MG tumors receiving  $^{177}\text{Lu}$ -3PRGD<sub>2</sub> were clearly visible at 4 h and 24 h p.i., with high contrast to the contralateral background (Fig 3A-B). Prominent gastrointestinal and renal uptake of this radiolabeled compound was also observed, suggesting both gastrointestinal and renal clearance of  $^{177}\text{Lu}$ -3PRGD<sub>2</sub>. Taken altogether, the imaging result was consistent with the biodistribution study.

### Safety of $^{177}\text{Lu}$ -3PRGD<sub>2</sub>

For the MTD determination, the animal body weight, WBC, RBC, HGB, PLA and GRN counts were analyzed after an escalating single injection dose of  $^{177}\text{Lu}$ -3PRGD<sub>2</sub> (Supplementary Material: Table S3, Fig 4). All those parameters showed a dose-dependent reduction. On day 9 p.i., these parameters reached the lowest level and then recovered to the baseline on day 16 p.i. (Fig 4). Overall, neither significant body weight loss (>20% of the original) nor mortality was observed in all groups. The highest dose (111 MBq) did not reach the MTD of  $^{177}\text{Lu}$ -3PRGD<sub>2</sub> in mice.

### Therapeutic efficacy of targeted radiotherapy and combined therapy

The therapeutic efficacy of  $^{177}\text{Lu}$ -3PRGD<sub>2</sub> was investigated in integrin  $\alpha_v\beta_3$ -positive U87MG tumor-bearing nude mice.  $^{177}\text{Lu}$ -3PRGD<sub>2</sub> possessed significant tumor inhibition effect as compared with the saline control group on day 28 post-treatment ( $P < 0.005$ , Fig 5A-B). From day 6, the mice receiving the 2  $\times$  111 MBq dose regimen of  $^{177}\text{Lu}$ -3PRGD<sub>2</sub> exhibited

the much better tumor growth inhibition as compared with the 111 MBq single dose ( $P < 0.001$  for day 6-14;  $P < 0.01$  for day 16-18;  $P < 0.05$  for day 20-26, Fig 5A).

The Endostar AAT was performed via peritumoral s.c. injection and intraperitoneal (i.p.) injection. Only the group administrated via peritumoral s.c. injection exhibited significant tumor inhibition effect as compared with the saline control group (Fig 5C-F, Supplementary Material: Fig S1). The tumor inhibition was further promoted by combining the  $^{177}\text{Lu}$ -3PRGD<sub>2</sub> TRT with Endostar AAT (peritumoral s.c. injection daily for two weeks), especially after day 18 (Fig 5C-D,  $P < 0.05$ ). No synergetic effect on tumor growth inhibition was observed when the  $^{177}\text{Lu}$ -3PRGD<sub>2</sub> TRT combined with the Endostar AAT by i.p. injection (Supplementary Material: Fig S1C-D, S2D). As shown in Fig 5E-F, pretreatment with Endostar (s.c.) for 5 days before  $^{177}\text{Lu}$ -3PRGD<sub>2</sub> TRT didn't further improve the therapeutic efficacy, but exhibited a similar tumor inhibition effect as compared with the treatment group in which both

$^{177}\text{Lu}$ -3PRGD<sub>2</sub> TRT and Endostar AAT were initiated on day 0 (Fig 5E-F).

A dose-dependent reduction of body weight was observed, but no significant body weight loss (>20% of the original) was observed in all treatment groups (Supplementary Material: Fig S4).

### Immunofluorescence staining

CD31 and Ki67 immunofluorescence staining was performed to validate the therapeutic efficacy of  $^{177}\text{Lu}$ -3PRGD<sub>2</sub> and Endostar treatment. Consistent with the therapy data, the tumor vasculature and Ki67 positive area in the  $^{177}\text{Lu}$ -3PRGD<sub>2</sub> and Endostar treatment groups are much less than the control group, demonstrating the vasculature damage and the tumor cell proliferation inhibition of  $^{177}\text{Lu}$ -3PRGD<sub>2</sub>, as well as the neovascular growth inhibition of Endostar (Fig 6). Among the therapy groups, the repeated dose regimen and combination of  $^{177}\text{Lu}$ -3PRGD<sub>2</sub> and Endostar (s.c.) showed the best therapeutic efficacy.

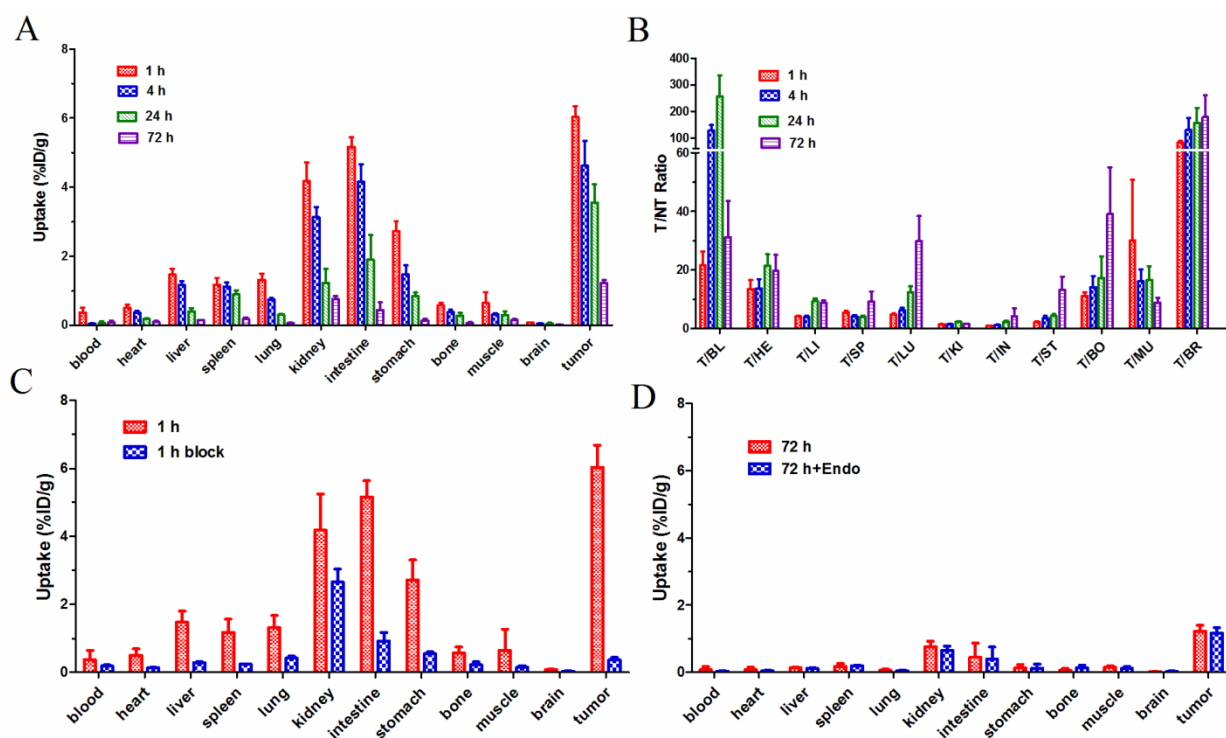


**Figure 2.** (A) Biodistribution of  $^{177}\text{Lu}$ -3PRGD<sub>2</sub> in U87MG tumor-bearing nude mice at 1 h, 4 h, 24 h, and 72 h after injection (370 kBq per mouse). (B) T/NT ratios of  $^{177}\text{Lu}$ -3PRGD<sub>2</sub> in U87MG tumor-bearing nude mice at 1 h, 4 h, 24 h, and 72 h after injection (370 kBq per mouse). (C) Comparison of biodistribution of  $^{177}\text{Lu}$ -3PRGD<sub>2</sub> with/without cold peptide blocking in U87MG tumor-bearing nude mice at 1 h after injection (370 kBq per mouse). (D) Comparison of biodistribution of  $^{177}\text{Lu}$ -3PRGD<sub>2</sub> with/without Endostar treatment in U87MG tumor-bearing nude mice at 72 h after injection (370 kBq per mouse). Data are expressed as means  $\pm$  SD (n = 4 per group).

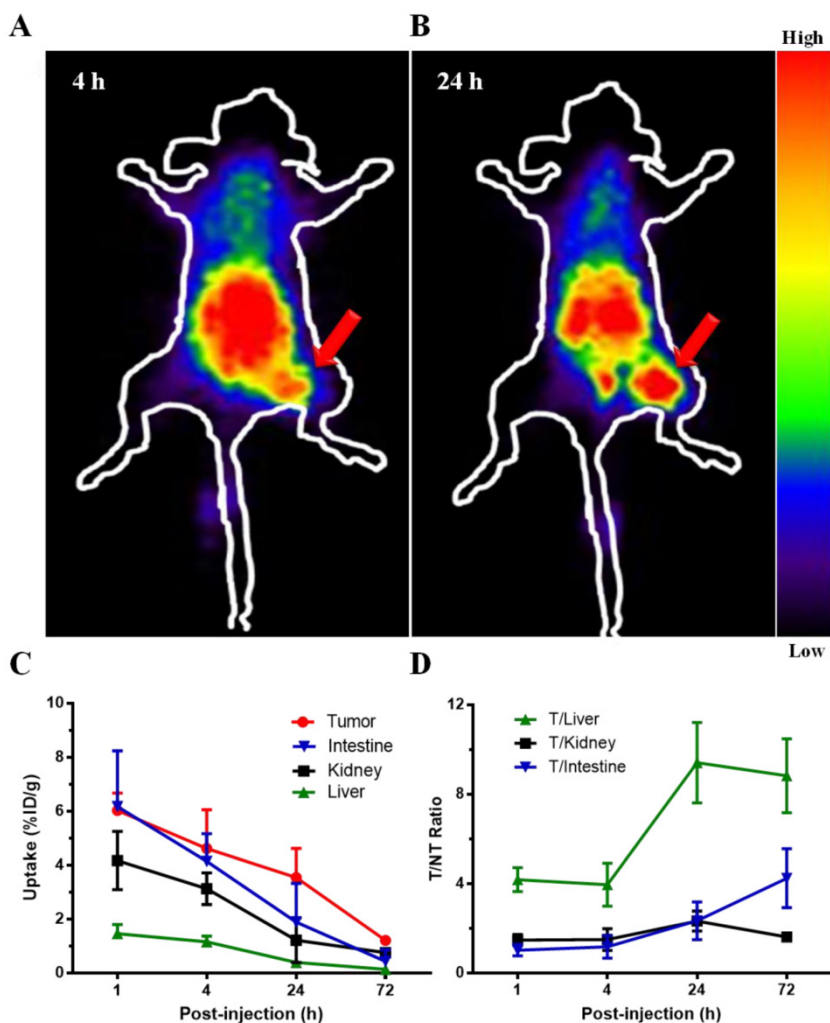


**Figure 3.** Representative planar gamma images of U87MG tumor-bearing nude mice at 4 h and 24 h after intravenous injection of ~74 MBq of <sup>177</sup>Lu-3PRGD<sub>2</sub>. (n = 3 per group). Tumors are indicated by arrows.

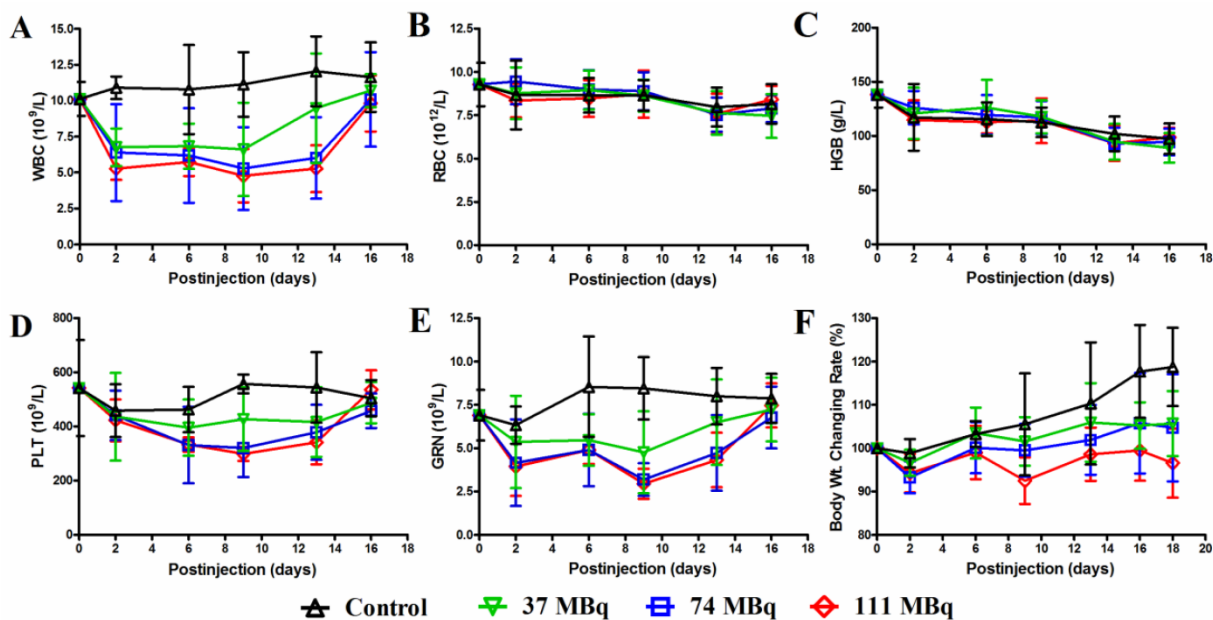


**Figure 4.** A MTD study was completed using escalating <sup>177</sup>Lu-3PRGD<sub>2</sub> doses of 0, 37, 74 and 111 MBq. Each dose was tested in seven female BALB/c nude mice. A hematology profile was measured twice-weekly, including (A) white blood cell (WBC), (B) red blood cell (RBC), (C) hemoglobin (HGB), (D) platelet (PLT), (E) neutrophil granulocyte (GRN). (F) Body weight was measured every other day.

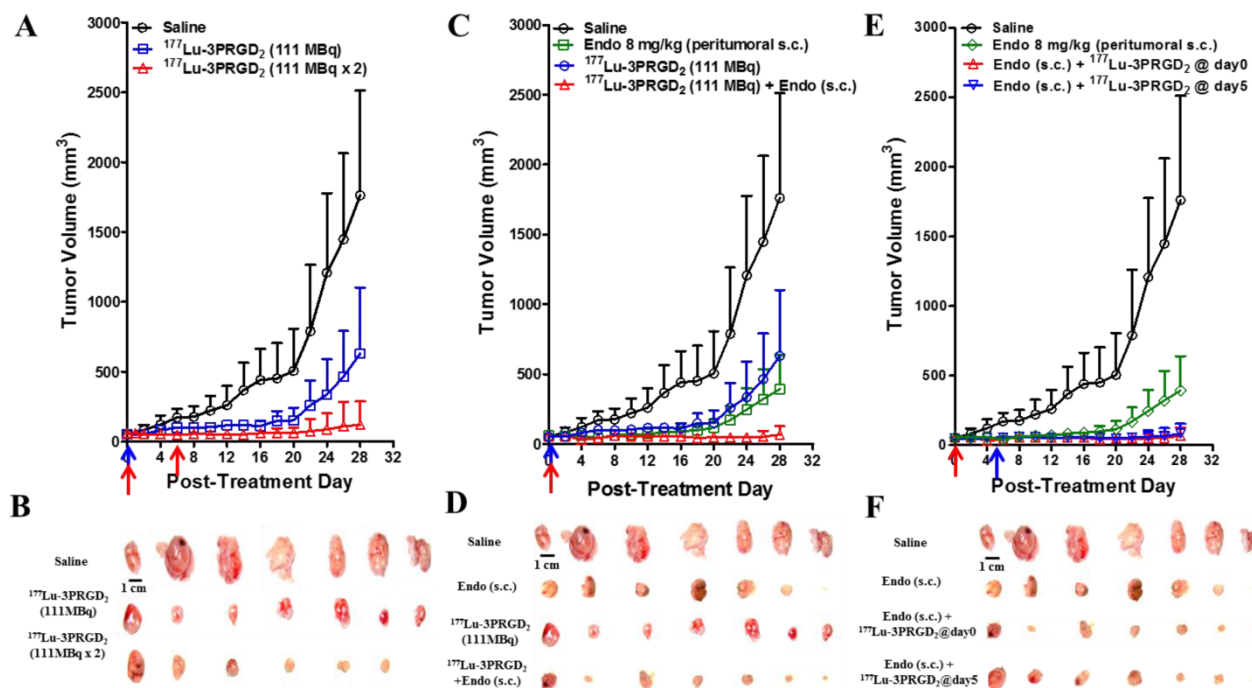


**Figure 5.** (A) Radionuclide therapy of established U87MG tumor in nude mice with saline (as control), <sup>177</sup>Lu-3PRGD<sub>2</sub> single dose (111 MBq), or <sup>177</sup>Lu-3PRGD<sub>2</sub> two doses (111 MBq × 2 on day 0 and day 6, respectively). (B) Tumor pictures of groups in (A) at the end of treatment. (C) Combination therapy of established U87MG tumors in nude mice with saline (as control), Endostar (8 mg/kg, peritumoral subcutaneous injection), <sup>177</sup>Lu-3PRGD<sub>2</sub> (111 MBq), or <sup>177</sup>Lu-3PRGD<sub>2</sub> (111 MBq) + Endostar (8 mg/kg, peritumoral subcutaneous injection). (D) Tumor pictures of groups in (C) at the end of treatment. (E) Combination therapy of established U87MG tumors in nude mice with saline (as control), Endostar (8 mg/kg, peritumoral subcutaneous injection), Endostar (8 mg/kg, (s.c.) peritumoral subcutaneous injection) + <sup>177</sup>Lu-3PRGD<sub>2</sub> (111 MBq day 0), or Endostar (8 mg/kg, peritumoral subcutaneous injection) + <sup>177</sup>Lu-3PRGD<sub>2</sub> (111 MBq day 5). (F) Tumor pictures of groups in (E) at the end of treatment. The time point of radioactivity administration was indicated by an arrow. Volume of tumors in each treatment group was measured and expressed as a function of time (means ± SD, n = 7 per group).

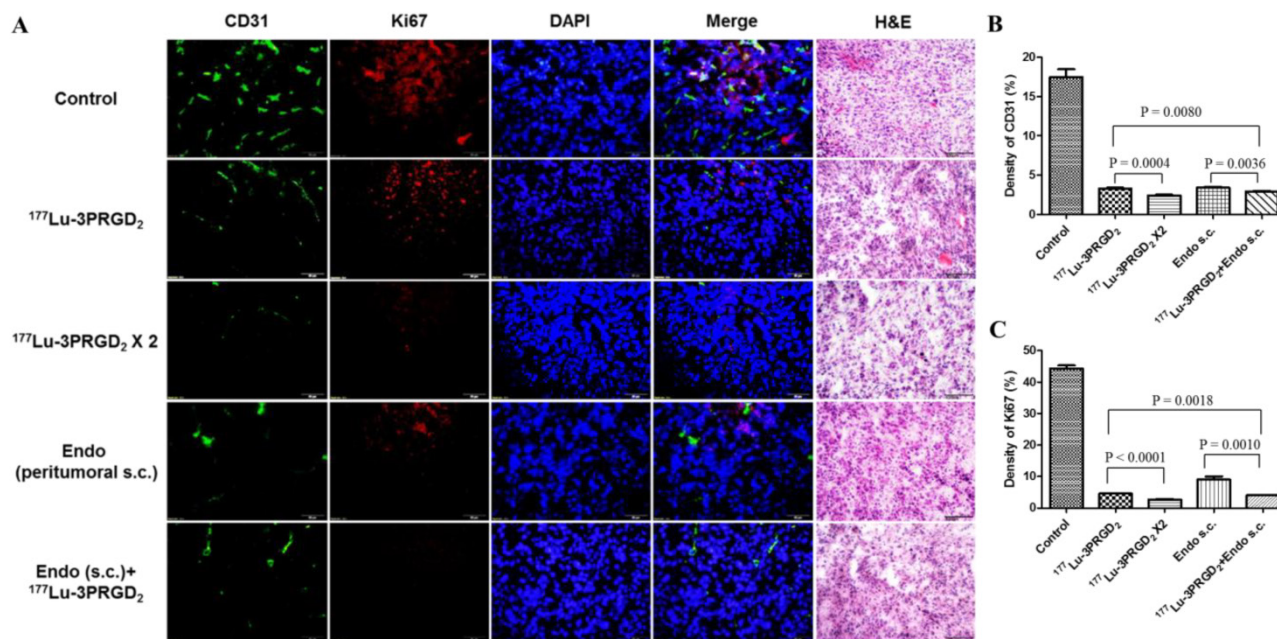


**Figure 6.** A) CD31 (green), Ki67 (red), DAPI (blue) staining and Hematoxylin-Eosin (H&E) staining of the frozen U87MG tumor tissue slices at the end of treatment with saline (as control), <sup>177</sup>Lu-3PRGD<sub>2</sub> (111 MBq), <sup>177</sup>Lu-3PRGD<sub>2</sub> (111 MBq × 2), Endostar (8 mg/kg, peritumoral subcutaneous injection) and <sup>177</sup>Lu-3PRGD<sub>2</sub> (111 MBq) + Endostar (8 mg/kg, peritumoral subcutaneous injection). B) Density of CD31 was analyzed by Image J software, C) Density of Ki67 was analyzed by Image J software.

## Discussion

The physical properties of  $^{177}\text{Lu}$  offer advantages compared to  $^{90}\text{Y}$ .  $^{177}\text{Lu}$  emits low energy  $\gamma$ -rays which directly allow quantitative determination of the biodistribution and dosimetry as well as the  $\gamma$ -imaging of the  $^{177}\text{Lu}$ -labeled tracers without using a radionuclide surrogate. In addition,  $^{177}\text{Lu}$  has shorter tissue penetration range ( $R_{\text{max}}$ : 2 mm) and relatively mild  $\beta$ -emission ( $E_{\text{max}}$ : 0.497 MeV), which is favorable for treatment of small tumors and micrometastases, and offers the advantage of lower irradiation of normal tissues adjacent to the tumors (37, 38). Thus,  $^{177}\text{Lu}$ -labeled peptides are more suitable for high dose and multiple-dose regimens. Given the promising glioblastoma growth inhibition by the targeted  $^{90}\text{Y}$ -3PRGD<sub>2</sub> radionuclide therapy in our previous study (24),  $^{177}\text{Lu}$  was employed in this study to introduce higher dose and multiple-dose regimens, which successfully improved the tumor inhibition efficacy.

Since the efficacy of TRT mainly depends on the specific accumulation of radiation in tumor, the tumor uptake and tumor-to-non-tumor (T/NT) ratios are crucial for a therapeutic agent. Here, we compared the biodistribution data of  $^{177}\text{Lu}$ -3PRGD<sub>2</sub> with  $^{111}\text{In}$ -3PRGD<sub>2</sub>/ $^{111}\text{In}$ -RGD<sub>4</sub> (as the surrogates of  $^{90}\text{Y}$ -3PRGD<sub>2</sub>/ $^{90}\text{Y}$ -RGD<sub>4</sub>). As  $^{90}\text{Y}$  is a pure  $\beta$  nuclide, biodistribution and imaging for  $^{90}\text{Y}$ -labeled agents are usually estimated using  $^{111}\text{In}$ -labeled corresponding agents, which is biologically equivalent to  $^{90}\text{Y}$ -labeled agents (24). The tumor uptake of  $^{177}\text{Lu}$ -3PRGD<sub>2</sub> at later time points ( $3.5 \pm 1.1$  %ID/g and  $1.2 \pm 0.2$  %ID/g at 24 and 72 h p.i. respectively) was slightly higher than  $^{111}\text{In}$ -3PRGD<sub>2</sub> (as the surrogate of  $^{90}\text{Y}$ -3PRGD<sub>2</sub>) ( $2.03 \pm 0.24$  %ID/g and  $0.45 \pm 0.05$  %ID/g) and more comparable to  $^{111}\text{In}$ -RGD<sub>4</sub> (as the surrogate of  $^{90}\text{Y}$ -RGD<sub>4</sub>) ( $3.67 \pm 0.57$  %ID/g and  $1.72 \pm 0.41$  %ID/g), providing stronger and longer radiation treatment. Moreover, the uptake of  $^{177}\text{Lu}$ -3PRGD<sub>2</sub> in normal organs, especially kidneys ( $4.2 \pm 1.1$  %ID/g and  $3.1 \pm 0.6$  %ID/g at 1 h and 4 h p.i., respectively), was much lower than that of  $^{111}\text{In}$ -RGD<sub>4</sub> ( $13.23 \pm 1.22$  %ID/g and  $10.99 \pm 0.88$  %ID/g) (24), which resulted in much higher T/NT ratios and possibly much lower toxicity, indicating the desirable properties of this therapeutic agent (Fig 1A-B and Fig 2C-D). Thus, with the advantage of the relative long half-life (2.67 d) of  $^{177}\text{Lu}$ , the very high and potentially tumoricidal accumulated absorbed doses could be achieved.

Imaging and dosimetry before and during therapy are very valuable for the treatment planning and for the evaluation of the outcome. However, the dosimetric data on radiolabeled 3PRGD<sub>2</sub> are still rare. For the first time, the human absorbed doses to nor-

mal organs for  $^{177}\text{Lu}$ -3PRGD<sub>2</sub> were estimated from biodistribution data in U87MG tumor-bearing mice by using a dedicated software (OLINDA/EXM) (Table 2). It shows much lower whole body absorbed doses ( $0.014 \pm 0.004$  mSv/MBq) than  $^{177}\text{Lu}$ -DOTA-Y<sup>3</sup>-TATE ( $0.031 \pm 0.007$  mSv/MBq) (39), which has been currently using in clinic. The  $\gamma$ -imaging of  $^{177}\text{Lu}$ -3PRGD<sub>2</sub> in U87MG tumors revealed high tumor uptake and fast clearance from liver, kidneys and intestine, which was consistent with the biodistribution data. With this imaging potential, the  $^{177}\text{Lu}$ -3PRGD<sub>2</sub> could be not only used for TRT, but also used as imaging diagnosis agent for screening patients before personalized TRT and guiding the treatment (37, 38).

Hematological parameters and body weight loss were used as the gross toxicity criteria in the MTD study. The mice exhibited much higher tolerance to  $^{177}\text{Lu}$ -3PRGD<sub>2</sub> ( $>55.5$  GBq/kg or 150 mCi/kg) as compared with  $^{90}\text{Y}$ -3PRGD<sub>2</sub> (27.7 GBq/kg or 75 mCi/kg), which was most likely due to its relatively mild  $\beta$ -emission inducing less irradiation in normal organs, especially in the kidneys and liver. The higher MTD of  $^{177}\text{Lu}$ -3PRGD<sub>2</sub> would allow higher single dose administration, and also possible treatment regimen of multiple doses.

Radiolabeled RGD peptides can specifically bind integrin  $\alpha_v\beta_3$  expressed both on tumor cell surface and the new-born tumor vasculature (38), therefore,  $^{177}\text{Lu}$ -labeled RGD peptides are considered to specifically deliver radiotherapeutics to both the integrin  $\alpha_v\beta_3$ -expressing tumor cells and the tumor neovasculature, which may lead to better management of solid tumors. In our radionuclide therapy studies, partial tumor regression was successfully achieved by a single dose of 111 MBq  $^{177}\text{Lu}$ -3PRGD<sub>2</sub>, and the therapeutic effect of  $^{177}\text{Lu}$ -3PRGD<sub>2</sub> was significantly better than that of control group (Fig 5A-B, S2A), while the tumor volume doubling time (TVDT) was 11 days and 3 days, respectively (Table 1). Due to the higher MTD and longer tumor radiation retention,  $^{177}\text{Lu}$ -3PRGD<sub>2</sub> possessed more gratifying tumor regression effect as compared with  $^{90}\text{Y}$ -3PRGD<sub>2</sub> at well-tolerated doses (TVDT: 11 days vs. 7 days, Table 1) (24). Yoshimoto M. *et al.* reported that multiple-dose administration ( $11.1$  MBq  $\times$  3) of  $^{90}\text{Y}$ -DOTA-c(RGDfK) (RGD monomer) induced more significant inhibition of tumor growth than single dose injection (TVDT: 12 days vs. 10 days) (40). Considering the less toxicity of  $^{177}\text{Lu}$ -3PRGD<sub>2</sub>, the higher or multiple-dose injection of  $^{177}\text{Lu}$ -3PRGD<sub>2</sub> is speculated to be more effective for tumor therapy. We also investigated the repeated dose administration of  $^{177}\text{Lu}$ -3PRGD<sub>2</sub> in U87MG tumor model, and the second dose was administrated on day 6 with the interval as one half-life of  $^{177}\text{Lu}$ . Two

cycles of <sup>177</sup>Lu-3PRGD<sub>2</sub> administration significantly increased the anti-tumor effect as compared with the single dose (TVDT: 28 days vs. 11 days), which is more pronounced compared with (11.1 MBq × 3) of <sup>90</sup>Y-DOTA-c(RGDfK) (TVDT: 28 days vs.12 days), even remarkably cured one tumor among 7 tumors (Fig 5A-B, S2A, Table 1). Since the single dose TRT showed notable tumor regression until day 20, the two dose regimen might be optimized by extending dosing interval to 20 days to get prolonged therapy efficacy. It could be further improved by introducing more repeated doses in the multiple dose regimen as well. The vasculature destruction and tumor cell proliferation inhibition of <sup>177</sup>Lu-3PRGD<sub>2</sub> TRT resulted in the reduced tumor vasculature and tumor growth inhibition, which were confirmed by CD31 and Ki67 staining. Both CD31<sup>+</sup> vascular endothelial cells and Ki67 positive areas showed significant reduction, suggesting <sup>177</sup>Lu-3PRGD<sub>2</sub> treatment induced vasculature collapse and tumor regression (Fig 6). These findings were also confirmed by H&E staining results, which showed more structural damages in tumor tissue of the TRT treatment group (Fig 6).

Endostar, as an endogenous inhibitor of angiogenesis, has been verified to combine with standard chemotherapy or radiation therapy regimens to improve the tumor regression (30, 31, 41). Zhou J. et al. reported that combining Endostar with external beam radiotherapy successfully improved the inhibition of the NPC (Nasopharyngeal carcinoma) xenograft tumor growth and increased the sensitivity of tumor cells to radiation (30). In the current study, the cross-influence of Endostar injection to <sup>177</sup>Lu-3PRGD<sub>2</sub> tumor uptake was firstly evaluated. As a result, the tumor uptake was found non-affected during the Endostar treatment (Fig 2D). The results insured that <sup>177</sup>Lu-3PRGD<sub>2</sub> and Endostar could be used as a combination therapy. The tumor growth was significantly inhibited only by administrating Endostar via peritumoral s.c. injection, possibly due to the poor concentration of Endostar dose in U87MG tumor by systemic administration (TVDT: 21 days vs. 5 days) (Supplementary Material: Fig S1, S2C-D, Table 1), which also has been proved by Schmidt group (28). Combination therapy of <sup>177</sup>Lu-3PRGD<sub>2</sub> TRT and Endostar (s.c.) further improved the tumor regression, which was more notable starting from day 18 than the mono-therapy with <sup>177</sup>Lu-3PRGD<sub>2</sub> or Endostar (s.c.), and the TVDT was remarkably prolonged to more than 28 days (Fig 5C-D, S2B, Table 1; *P* < 0.05). Also, the vasculature destruction and tumor cell proliferation inhibition of AAT and combination therapy were confirmed by CD31 and Ki67 staining, which showed significantly reduced CD31<sup>+</sup> vascular endothelial cells and Ki67 positive areas, suggesting vasculature col-

lapse and tumor regression (Fig 6). These findings were also confirmed by H&E staining results, which showed more structural damages in the tumor tissues of the combination treatment group.

**Table 1.** Tumor volume doubling time of all experimental groups in therapy studies.

Experimental groups	Tumor volume doubling time (days)
Control	3
Cold peptide (~5 µg @ day 0)*	3
<sup>177</sup> Lu-3PRGD <sub>2</sub> (111 MBq @ day 0)	11
<sup>177</sup> Lu-3PRGD <sub>2</sub> (111 MBq × 2 @ day 0 and day 6)	28
Endostar treatment (i.p. 8 mg/kg/day for two weeks)#	5
<sup>177</sup> Lu-3PRGD <sub>2</sub> + Endostar (i.p.)#	15
Endostar treatment (peritumoral s.c.)	21
<sup>177</sup> Lu-3PRGD <sub>2</sub> + Endostar (peritumoral s.c.)	>28
<sup>90</sup> Y-3PRGD <sub>2</sub> (37 MBq @ day 0)*	7
<sup>90</sup> Y-3PRGK <sub>2</sub> (37 MBq @ day 0)*	4
<sup>90</sup> Y-RGD <sub>4</sub> (37 MBq @ day 0)*	6
<sup>90</sup> Y-RGD <sub>4</sub> (18.5 MBq @ day 0)*	3
<sup>90</sup> Y-RGD <sub>4</sub> (18.5 MBq × 2 @ day 0 and day 6)*	5

Note:  
 #: data showed in supplementary material (Fig S1-2).  
 \*: data from previous paper (24). The 3PRGK<sub>2</sub> is a nonsense counterpart of 3PRGD<sub>2</sub>.  
 Endostar treatment was administrated at 8 mg/kg daily for two weeks via either i.p. or peritumoral s.c. route.  
 All the single dose of <sup>177</sup>Lu-3PRGD<sub>2</sub> (111 MBq) in combination therapy was administrated on day 0.

**Table 2.** Human absorbed dose estimates of <sup>177</sup>Lu-3PRGD<sub>2</sub> obtained from U87MG tumor mice.

Target Organ	Effective Dose (mSv/MBq)		
	Mean	SD	N
Adrenals	3.36E-06	3.08E-07	4
Brain	2.83E-06	5.24E-07	4
Breasts	1.29E-05	5.52E-06	4
LLI Wall	3.92E-05	3.00E-05	4
Small Intestine	3.34E-06	4.02E-06	4
Stomach Wall	2.11E-04	1.88E-04	4
ULI Wall	3.46E-06	3.25E-06	4
Heart Wall	7.75E-04	1.54E-04	4
Kidneys	7.39E-04	2.21E-04	4
Liver	7.77E-04	1.21E-04	4
Lungs	2.52E-03	4.58E-04	4
Muscle	2.20E-06	4.73E-07	4
Pancreas	4.18E-06	5.26E-07	4
Red Marrow	5.25E-05	1.08E-05	4
Osteogenic Cells	8.75E-05	3.10E-05	4
Skin	1.86E-06	7.74E-07	4
Spleen	5.81E-03	1.19E-03	4
Thymus	8.92E-07	3.52E-07	4
Thyroid	9.02E-06	4.49E-06	4
Urinary Bladder Wall	9.26E-06	7.49E-06	4
Total Body	1.35E-02	4.49E-03	4

Fang P. et al. (41) reported that Endostar could normalize the morphology and function of nasopharyngeal carcinoma (NPC) vasculature for a period of time, leading to transient improvement in tumor oxygenation and response to radiation therapy. According to their findings, the normalization window was mostly during the first treatment 5-7 days, which was proved in the U87MG tumor model by performing tumor IHC analysis with CD31 and NG-2 staining (Supplementary Material: Fig S3). NG-2 antibody was used to label pericytes around vascular, since increased pericyte coverage was considered as a key characteristics of tumor vessel normalization (41). As shown in Supplementary Material: Fig S3, the NG-2 positive area was found significantly enhanced at Endostar (s.c.) treatment on day 5 - 7, compared to untreated on day 0 and post-treatment day 14. However, the strategy that administrated Endostar 5 days in advance then combined with  $^{117}\text{Lu}$ -3PRGD<sub>2</sub> induced no further therapeutic improvement, compared with that both Endostar and  $^{117}\text{Lu}$ -3PRGD<sub>2</sub> were initiated at the day 0 (Fig 5E-F). More pretreatment studies with Endostar combined radiotherapy are still needed in the future to figure out if the normalization window theory would be suitable for TRT strategy. Other integrin  $\alpha_v\beta_3$ -positive tumor models and orthotopic tumor model should be involved in the further investigation. Our latest work of  $^{68}\text{Ga}$ -3PRGD<sub>2</sub> imaging for the orthotopic GBM has showed the feasibility to treat GBM orthotopic tumor with  $^{177}\text{Lu}$ -3PRGD<sub>2</sub> TRT (42).

Combination therapy showed comparable tumor growth inhibition to the two-dose TRT, but the latter does not need to repeat injection daily for weeks, which is more convenient and appreciative for clinical use. Given the favorable in vivo properties of  $^{177}\text{Lu}$ -3PRGD<sub>2</sub> and its promising tumor treatment efficacy in animal model, it could potentially be rapidly translated into clinical practice in the future.

## Conclusion

$^{177}\text{Lu}$ -3PRGD<sub>2</sub> exhibited high specific tumor targeting properties and relatively low uptake in normal organs, especially in kidneys and liver, leading to relatively low toxicity and higher MTD of  $^{177}\text{Lu}$ -3PRGD<sub>2</sub>, comparing with  $^{90}\text{Y}$ -3PRGD<sub>2</sub>. The high MTD of  $^{177}\text{Lu}$ -3PRGD<sub>2</sub> made it more suitable for high dose or multiple-dose regimens, so as to achieve maximum therapeutic efficacy. Either the repeated high-dose regimen of  $^{177}\text{Lu}$ -3PRGD<sub>2</sub> or combination treatment of  $^{177}\text{Lu}$ -3PRGD<sub>2</sub> with Endostar potentially enhanced the tumor growth inhibition. Compared to Endostar combined treatment, the repeated  $^{177}\text{Lu}$ -3PRGD<sub>2</sub> does not need to inject daily for weeks, avoiding a lot of unnecessary inconvenience and suf-

fering for patients, which could potentially be rapidly translated into clinical practice in the future to improve the outcome of integrin  $\alpha_v\beta_3$ -positive tumor treatment in clinic.

## Abbreviations

**DOTA:** 1,4,7,10-tetraazacyclododecane-1,4,7,10-tetracetic acid;

**PEG<sub>4</sub>:** 15 amino-4,7,10,13-tetraoxapentadecanoic acid;

**c(RGDfK):** cyclo(Lys-Arg-Gly-Asp-D-Phe);

**E[c(RGDfK)]<sub>2</sub> (RGD<sub>2</sub>):** Glu[cyclo(Lys-Arg-Gly-Asp-D-Phe)-cyclo(Lys-Arg-Gly-Asp-D-Phe)];

**PEG<sub>4</sub>-E[PEG<sub>4</sub>-c(RGDfK)]<sub>2</sub> (3PRGD<sub>2</sub>):** PEG<sub>4</sub>-Glu{cyclo[Lys(PEG<sub>4</sub>)-Arg-Gly-Asp-D-Phe]-cyclo[Lys(PEG<sub>4</sub>)-Arg-Gly-Asp-D-Phe]};

**PEG<sub>4</sub>-E[PEG<sub>4</sub>-c(RGKfD)]<sub>2</sub> (3PRGK<sub>2</sub>):** PEG<sub>4</sub>-Glu{cyclo[Arg-Gly-Lys(PEG<sub>4</sub>)-D-Phe-Asp]-cyclo[Arg-Gly-Lys(PEG<sub>4</sub>)-D-Phe-Asp]};

**E[E[c(RGDfK)]<sub>2</sub>]<sub>2</sub> (RGD<sub>4</sub>):** Glu{Glu[cyclo(Lys-Arg-Gly-Asp-D-Phe)]-cyclo(Lys-Arg-Gly-Asp-D-Phe)}-Glu{cyclo(Lys-Arg-Gly-Asp-D-Phe)-cyclo(Lys-Arg-Gly-Asp-D-Phe)}.

## Supplementary Material

Methods, Table S1-S2, Figure S1-S4.

<http://www.thno.org/v04p0256s1.pdf>

## Acknowledgment

This work was financially supported, in part, by the Outstanding Youth Fund (81125011), "973" program (2013CB733802 and 2011CB707703), National Natural Science Foundation of China (NSFC) projects (81000625, 30930030, 81222019, 30900373, 81201127, 81028009 and 81321003), grants from the Ministry of Science and Technology of China (2012ZX09102301-018, 2011YQ030114, and 2012BAK25B03-16), and grants from the Ministry of Education of China (31300 and BMU20110263).

## Competing Interests

The authors have declared that no competing interest exists.

## References

- Begg AC, Stewart FA, Vens C. Strategies to improve radiotherapy with targeted drugs. *Nature reviews Cancer*. 2011;11:239-53.
- Delaney G, Jacob S, Featherstone C, Barton M. The role of radiotherapy in cancer treatment: estimating optimal utilization from a review of evidence-based clinical guidelines. *Cancer*. 2005;104:1129-37.
- Fani M, Maecke HR, Okarvi SM. Radiolabeled peptides: valuable tools for the detection and treatment of cancer. *Theranostics*. 2012;2:481-501.
- Ersahin D, Doddamani I, Cheng D. Targeted Radionuclide Therapy. *Cancers*. 2011;3:3838-55.
- Veeravagu A, Liu Z, Niu G, Chen K, Jia B, Cai W, et al. Integrin v 3-Targeted Radioimmunotherapy of Glioblastoma Multiforme. *Clinical Cancer Research*. 2008;14:7330-9.
- Miederer M, Henriksen G, Alke A, Mossbrugger I, Quintanilla-Martinez L, Senekowitsch-Schmidtke R, et al. Preclinical Evaluation of the  $\alpha_v\beta_3$ -Particle

- Generator Nuclide 225Ac for Somatostatin Receptor Radiotherapy of Neuroendocrine Tumors. *Clinical Cancer Research*. 2008;14:3555-61.
7. Kwekkeboom DJ, de Herder WW, Kam BL, van Eijck CH, van Essen M, Kooij PP, et al. Treatment With the Radiolabeled Somatostatin Analog [177Lu-DOTA0,Tyr3]Octreotate: Toxicity, Efficacy, and Survival. *Journal of Clinical Oncology*. 2008;26:2124-30.
  8. Liu Z, Wang F, Chen X. Integrin alpha(v)beta(3)-Targeted Cancer Therapy. *Drug development research*. 2008;69:329-39.
  9. Danhier F, Breton AL, Pr at V. RGD-Based Strategies To Target Alpha(v) Beta(3) Integrin in Cancer Therapy and Diagnosis. *Molecular Pharmaceutics*. 2012;121004113049007.
  10. Liu Z WF, and Chen X. Integrin Targeted Delivery of Radiotherapeutics. *Theranostics*. 2011;1:10.
  11. Beer AJ, Schwaiger M. Imaging of integrin alphavbeta3 expression. *Cancer metastasis reviews*. 2008;27:631-44.
  12. Yin Zhang YY, Weibo Cai. Multimodality Imaging of Integrin  $\alpha v \beta 3$  Expression. *Theranostics*. 2011;1:13.
  13. Gaertner FC, Kessler H, Wester HJ, Schwaiger M, Beer AJ. Radiolabelled RGD peptides for imaging and therapy. *European Journal of Nuclear Medicine and Molecular Imaging*. 2012;39:126-38.
  14. Shi J, Liu Z, Jia B, Yu Z, Zhao H, Wang F. Potential therapeutic radiotracers: preparation, biodistribution and metabolic characteristics of 177Lu-labeled cyclic RGDfK dimer. *Amino Acids*. 2009;39:111-20.
  15. Shi J, Zhou Y, Chakraborty S, et al. Evaluation of 111In-Labeled Cyclic RGD Peptides: Effects of Peptide and Linker Multiplicity on Their Tumor Uptake, Excretion Kinetics and Metabolic Stability. *Theranostics*. 2011;1:18.
  16. Janssen ML, Oyen WJ, Dijkgraaf I, Massuger LF, Frielink C, Edwards DS, et al. Tumor targeting with radiolabeled alpha(v)beta(3) integrin binding peptides in a nude mouse model. *Cancer Res*. 2002;62:6146-51.
  17. Sudipta Chakraborty JS, Young-Seung Kim, Yang Zhou, Bing Jia, Fan Wang, and Shuang Liu. Evaluation of 111In-Labeled Cyclic RGD Peptides: Tetrameric not Trivalent. *Bioconjugate Chem*. 2010;21:10.
  18. Wu Y, Zhang X, Xiong Z, Cheng Z, Fisher DR, Liu S, et al. microPET imaging of glioma integrin  $\{\alpha\}v\{\beta\}3$  expression using  $^{64}\text{Cu}$ -labeled tetrameric RGD peptide. *J Nucl Med*. 2005;46:1707-18.
  19. Li ZB, Cai W, Cao Q, Chen K, Wu Z, He L, et al.  $^{64}\text{Cu}$ -labeled tetrameric and octameric RGD peptides for small-animal PET of tumor alpha(v)beta(3) integrin expression. *J Nucl Med*. 2007;48:1162-71.
  20. Liu Z, Liu S, Wang F, Liu S, Chen X. Noninvasive imaging of tumor integrin expression using  $^{18}\text{F}$ -labeled RGD dimer peptide with PEG<sub>4</sub> linkers. *Eur J Nucl Med Mol Imaging*. 2009;36:1296-307.
  21. Shi J, Wang L, Kim YS, Zhai S, Liu Z, Chen X, et al. Improving tumor uptake and excretion kinetics of  $^{99\text{m}}\text{Tc}$ -labeled cyclic arginine-glycine-aspartic (RGD) dimers with triglycine linkers. *J Med Chem*. 2008;51:7980-90.
  22. Shi J, Kim YS, Zhai S, Liu Z, Chen X, Liu S. Improving tumor uptake and pharmacokinetics of  $^{64}\text{Cu}$ -labeled cyclic RGD peptide dimers with Gly<sub>3</sub> and PEG<sub>4</sub> linkers. *Bioconjug Chem*. 2009;20:750-9.
  23. Liu Z, Jia B, Shi J, Jin X, Zhao H, Li F, et al. Tumor Uptake of the RGD Dimeric Probe  $^{99\text{m}}\text{Tc}$ -G3-2P4-RGD2 is Correlated with Integrin  $\alpha v \beta 3$  Expressed on both Tumor Cells and Neovasculature. *Bioconjugate Chem*. 2010;21:548-55.
  24. Liu Z, Shi J, Jia B, Yu Z, Liu Y, Zhao H, et al. Two $^{90\text{Y}}$ -Labeled Multimeric RGD Peptides RGD4 and 3PRGD2 for Integrin Targeted Radionuclide Therapy. *Molecular Pharmaceutics*. 2011;8:591-9.
  25. Ma Q, Ji B, Jia B, Gao S, Ji T, Wang X, et al. Differential diagnosis of solitary pulmonary nodules using  $^{99\text{m}}\text{Tc}$ -3P(4)-RGD(2) scintigraphy. *Eur J Nucl Med Mol Imaging*. 2011;38:2145-52.
  26. Zhao D, Jin X, Li F, Liang J, Lin Y. Integrin alphavbeta3 Imaging of Radioactive Iodine-Refractory Thyroid Cancer Using  $^{99\text{m}}\text{Tc}$ -3PRGD2. *J Nucl Med*. 2012.
  27. Zhu Z, Miao W, Li Q, Dai H, Ma Q, Wang F, et al.  $^{99\text{m}}\text{Tc}$ -3PRGD2 for integrin receptor imaging of lung cancer: a multicenter study. *J Nucl Med*. 2012;53:716-22.
  28. Schmidt NO, Ziu M, Carrabba G, Giussani C, Bello L, Sun Y, et al. Antiangiogenic therapy by local intracerebral microinfusion improves treatment efficiency and survival in an orthotopic human glioblastoma model. *Clinical cancer research : an official journal of the American Association for Cancer Research*. 2004;10:1255-62.
  29. Luna-Guti rrez M, Ferro-Flores G, Ocampo-Garc a B, Jim enez-Mancilla N, Morales-Avila E, De Le n-Rodr guez L, et al. 177Lu-labeled monomeric, dimeric and multimeric RGD peptides for the therapy of tumors expressing  $\alpha(v)\beta(3)$  integrins. *Journal of Labelled Compounds and Radiopharmaceutics*. 2012;55:140-8.
  30. Ke Q-H, Zhou S-Q, Huang M, Lei Y, Du W, Yang J-Y. Early Efficacy of Endostar Combined with Chemoradiotherapy for Advanced Cervical Cancers. *Asian Pacific Journal of Cancer Prevention*. 2012;13:923-6.
  31. Chamberlain MC, Cloughsey T, Reardon DA, Wen PY. A novel treatment for glioblastoma: integrin inhibition. *Expert review of neurotherapeutics*. 2012;12:421-35.
  32. Lee JH, Song JH, Lee SN, Kang JH, Kim MS, Sun DJ, et al. Adjuvant Postoperative Radiotherapy with or without Chemotherapy for Locally Advanced Squamous Cell Carcinoma of the Head and Neck: The Importance of Patient Selection for the Postoperative Chemoradiotherapy. *Cancer research and treatment : official journal of Korean Cancer Association*. 2013;45:31-9.
  33. Lee FT, Mountain AJ, Kelly MP, Hall C, Rigopoulos A, Johns TG, et al. Enhanced efficacy of radioimmunotherapy with  $^{90\text{Y}}$ -CHX-A"-DTPA-hu3S193 by inhibition of epidermal growth factor receptor (EGFR) signaling with EGFR tyrosine kinase inhibitor AG1478. *Clinical cancer research : an official journal of the American Association for Cancer Research*. 2005;11:7080s-6s.
  34. Dumont RA, Tamma M, Braun F, Borkowski S, Reubi JC, Maecke H, et al. Targeted radiotherapy of prostate cancer with a gastrin-releasing peptide receptor antagonist is effective as monotherapy and in combination with rapamycin. *J Nucl Med*. 2013;54:762-9.
  35. Liang J, E M, Wu G, Zhao L, Li X, Xiu X, et al. Nimotuzumab combined with radiotherapy for esophageal cancer: preliminary study of a Phase II clinical trial. *OncoTargets and therapy*. 2013;6:1589-96.
  36. Robertson R, Germanos MS, Manfredi MG, Smith PG, Silva MD. Multimodal imaging with  $^{18}\text{F}$ -FDG PET and Cerenkov luminescence imaging after MLN4924 treatment in a human lymphoma xenograft model. *J Nucl Med*. 2011;52:1764-9.
  37. Brans B, Mottaghy FM, Kessels A.  $^{90\text{Y}}$ /177Lu-DOTATATE therapy: survival of the fittest? *Eur J Nucl Med Mol Imaging*. 2011;38:1785-7.
  38. Kwekkeboom DJ, Kam BL, van Essen M, Teunissen JJ, van Eijck CH, Valkema R, et al. Somatostatin-receptor-based imaging and therapy of gastroenteropancreatic neuroendocrine tumors. *Endocrine-related cancer*. 2010;17:R53-73.
  39. Lewis JS WM, Laforest R, Wang F, Erion JL, Bugaj JE, Srinivasan A, Anderson CJ. Toxicity and dosimetry of  $^{177}\text{Lu}$ -DOTA-Y3-octreotate in a rat model. *Int J Cancer*. 2001;94:5.
  40. Yoshimoto M, Ogawa K, Washiyama K, Shikano N, Mori H, Amano R, et al. alpha(v)beta(3) Integrin-targeting radionuclide therapy and imaging with monomeric RGD peptide. *Int J Cancer*. 2008;123:709-15.
  41. Peng F, Xu Z, Wang J, Chen Y, Li Q, Zuo Y, et al. Recombinant human endostatin normalizes tumor vasculature and enhances radiation response in xenografted human nasopharyngeal carcinoma models. *PLoS one*. 2012;7:e34646.
  42. Shi J, Fan D, Liu X, Yang L, Yan N, Sun Y, et al. Dual PET and Cerenkov luminescence imaging of a kit-formulated integrin  $\alpha v \beta 3$ -selective radiotracer  $^{68}\text{Ga}$ -3PRGD2 in human glioblastoma xenografts and orthotopic tumors. *Abstract Book Supplement to the Journal of Nuclear Medicine*. 2013;54:1.